QUALITY AND RELIABILITY ENGINEERING INTERNATIONAL
Qual. Reliab. Engng. Int. 2008; **24**:585–600
Published online 3 June 2008 in Wiley InterScience (www.interscience.wiley.com). DOI: 10.1002/qre.924

Research

A Bootstrap Control Chart for Birnbaum–Saunders Percentiles

Y. L. Lio[1] and Chanseok Park[2,*,†]

[1]*Department of Mathematical Sciences, University of South Dakota, Vermillion, SD 57069, U.S.A.*
[2]*Department of Mathematical Sciences, Clemson University, Clemson, SC 29634, U.S.A.*

The problem of detecting a shift in the percentile of a Birnbaum–Saunders population in a process monitoring situation is considered. For example, such problems may arise when the quality characteristic of interest is tensile strength or breaking stress. The parametric bootstrap method is used to develop a quality control chart for monitoring percentiles when process measurements have a Birnbaum–Saunders distribution. Through extensive Monte Carlo simulations, we investigate the behavior and performance of the proposed bootstrap percentile charts. Average run lengths of the proposed percentile chart are also investigated. Illustrative examples with the data concerning the tensile strength of the aluminum sheeting are presented.

Received 22 August 2007; Revised 29 January 2008; Accepted 10 April 2008

KEY WORDS: average run length; Birnbaum–Saunders distribution; control charts; false alarm rate; percentile; Shewhart chart; statistical process control; tensile strength

1. INTRODUCTION

The two-parameter Birnbaum–Saunders distributions have been shown to provide a better fit to strength or breaking stress data such as carbon fiber or composite tensile strengths than the more commonly used Weibull distributions by Durham and Padgett[1], in addition to cycles to failure data[2–4]. To our best knowledge, no control chart has been developed for monitoring the process that produces measurements of the Birnbaum–Saunders distribution. The well-known Shewhart $\bar{X}$ and R control charts assume that the observed process data come from a near-normal distribution. However, when the distribution of the process under observation is unknown or non-normal, the sampling distribution of a parameter estimator may not be available theoretically. In this case, the Shewhart-type charts are not available and computational methods, such as parametric or non-parametric bootstrap methods, can be used to set control limits for an appropriate control chart. See References[5–7] for a basic discussion of bootstrap techniques. An advantage of the bootstrap methods is that they are not restricted by assumptions on the distribution of the process measurements. The computation time of the method is perhaps a perceived disadvantage, but actually is not, given the current computing power available and considering the possibility of using an inappropriate control chart. In addition, with the advent of modern powerful and accessible computers, simulation-based estimation such as bootstrapping is much more easily and quickly obtained than before. The bootstrap method uses only the sample data to estimate the sampling distribution of the parameter estimator and then

*Correspondence to: Chanseok Park, Department of Mathematical Sciences, Clemson University, Clemson, SC 29634, U.S.A.
†E-mail: cspark@ces.clemson.edu

to determine appropriate control limits. Only the usual assumptions (for Phase II of the statistical process control paradigm), that the process is stable and subgroup observations are independent and identically distributed, are required.

In this paper, the problem of detecting a shift in the percentile of strength or breaking stress data such as carbon fiber or composite tensile strengths is considered. A minimum tensile strength of such materials is usually required for engineering design considerations and small percentiles are of interest. A downward shift in the lower percentile of the strength distribution indicates a decrease in the tensile strength. For an asymmetric distribution, when the quality characteristic of interest is a lower percentile and whose estimator has a non-normal distribution, the standard $\bar{X}$ and R Shewhart control charts may fail to detect important shifts in the specific lower percentile in question. This was discussed in detail by Padgett and Spurrier[8]. They developed Shewhart-type control charts for percentiles of Weibull or log-normal distributions using best linear invariant estimators (BLIEs) of the parameters for the control charts of Weibull percentiles. However, the pitfall of this approach is that it requires the tabled coefficients to obtain the BLIEs. In addition, as far as we know, the BLIEs for percentiles of the Birnbaum–Saunders distribution are not yet developed. Moreover, Nichols and Padgett[9] showed that the bootstrap control charts for Weibull percentiles could detect an out-of-control process earlier than the Shewhart-type control charts for Weibull percentiles. Therefore, the bootstrap-type charts will be constructed and used for monitoring the Birnbaum–Saunders percentile in this paper. The bootstrap charts, unlike the BLIEs, do not require the tabled coefficients in order to compute the percentiles of the Weibull distribution or the Birnbaum–Saunders distribution. It is noteworthy that Tagaras[10] and Marcellus[11] studied the advantage of using the Shewhart $\bar{X}$ chart with asymmetric control limits, but their assumed underlying distribution is normal.

The parametric bootstrap method is used to construct control chart limits for monitoring a specified percentile of the Birnbaum–Saunders distribution, which has been shown to provide a better fit to tensile strength or breaking stress data. Although the method works for any percentile, we are concerned specifically with small percentiles of the Birnbaum–Saunders distribution.

The procedure of constructing the parametric bootstrap control charts for Birnbaum–Saunders percentiles is presented in Section 3. In Section 4, the behavior and performance of the proposed bootstrap control limits for Birnbaum–Saunders percentiles are addressed through extensive Monte Carlo simulations, and an example of monitoring the breaking stress of the aluminum sheeting is given for illustration in Section 5. Finally, the concluding remarks are given in Section 6.

2. THE BIRNBAUM–SAUNDERS DISTRIBUTION

In this section, we give a brief introduction to the two-parameter Birnbaum–Saunders distribution and the estimations for the interesting quantities. This distribution was proposed by Birnbaum and Saunders[3]. Given the shape parameter $\alpha>0$ and scale parameter $\beta>0$, the probability density function and the cumulative distribution function (cdf) of the Birnbaum–Saunders distribution are typically given by

$$f(t)=\frac{1}{2\alpha\beta\sqrt{2\pi}}\left[\sqrt{\frac{\beta}{t}}+\left(\frac{\beta}{t}\right)^{3/2}\right]\exp\left[\frac{-1}{2\alpha^2}\left(\frac{t}{\beta}-2+\frac{\beta}{t}\right)\right]$$

and

$$F(t)=\Phi\left[\frac{1}{\alpha}\left(\sqrt{\frac{t}{\beta}}-\sqrt{\frac{\beta}{t}}\right)\right],\quad t>0$$

respectively, where $\Phi(\cdot)$ is the standard normal cdf. The maximum likelihood estimates (MLEs) of α and β were discussed originally by Birnbaum and Saunders[4]. It is noteworthy that the $100p$th percentile is given by $W_p=(\beta/4)[\alpha z_p+(\alpha^2 z_p^2+4)^{1/2}]^2$, where $z_p=\Phi^{-1}(p)$ is the standard normal $100p$th percentile.

DOI: 10.1002/qre

Let $\mathscr{T}=\{t_1, t_2, \ldots, t_n\}$ be a random sample of size n from the Birnbaum–Saunders distribution. A convenient method for obtaining the MLEs is as follows[12]. Let s and r be the sample arithmetic and harmonic means given by

$$s=\frac{1}{n}\sum_{i=1}^{n} t_i \quad \text{and} \quad r=\left[\frac{1}{n}\sum_{i=1}^{n} t_i^{-1}\right]^{-1}$$

Let $h(\cdot)$ be the harmonic mean function given by

$$h(\beta;\mathscr{T})=\left[\frac{1}{n}\sum_{i=1}^{n}(\beta+t_i)^{-1}\right]^{-1}$$

Then the MLE of β is obtained by solving the following estimating equation for β:

$$g(\beta;\mathscr{T})=\beta^2-\beta\{2r+h(\beta;\mathscr{T})\}+r\{s+h(\beta;\mathscr{T})\}=0 \tag{1}$$

It should be noted that in solving for β, the unique positive root lies in the interval (r, s). Two iterative methods for solving $g(\beta;\mathscr{T})=0$ are discussed by Birnbaum and Saunders[4]. However, these methods do not work properly in a certain range of the sample space[13]. Because the uniqueness of this solution is guaranteed in the interval (r, s), we use a one-dimensional root search in this paper instead of their methods. Once the MLE of β, denoted by $\hat{\beta}$, is obtained, the MLE of α, denoted by $\hat{\alpha}$, is explicitly obtained by computing

$$\hat{\alpha}=\sqrt{\frac{s}{\hat{\beta}}+\frac{\hat{\beta}}{r}-2} \tag{2}$$

Therefore, the MLE of the Birnbaum–Saunders percentile is $\hat{W}_p=(\hat{\beta}/4)[\hat{\alpha}z_p+(\hat{\alpha}^2z_p^2+4)^{1/2}]^2$.

Let T have the Birnbaum–Saunders distribution with parameters α and β; then T^{-1} has the Birnbaum–Saunders distribution with parameters α and β^{-1}. It can be shown that $E(T)=\beta(1+\frac{1}{2}\alpha^2)$ and $E(T^{-1})=\beta^{-1}(1+\frac{1}{2}\alpha^2)$. Equating $E(T)$ and $E(T^{-1})$ with the corresponding sample moments, Ng *et al.*[13] proposed the modified moment estimators (MMEs), $\tilde{\alpha}$ and $\tilde{\beta}$, for α and β, respectively, where

$$\tilde{\alpha}=\left[2\left(\frac{s}{r}\right)^{1/2}-2\right]^{1/2} \tag{3}$$

and

$$\tilde{\beta}=(sr)^{1/2} \tag{4}$$

Therefore, the Birnbaum–Saunders percentile can also be estimated by $\tilde{W}_p=(\tilde{\beta}/4)[\tilde{\alpha}z_p+(\tilde{\alpha}^2z_p^2+4)^{1/2}]^2$. Ng *et al.*[13] also proposed the corresponding bias-reduced MLEs and the corresponding bias-reduced MMEs and showed that the MLEs and MMEs behave very similarly. It should be noted that the bias corrections are for the estimators of α and β but not for percentile estimators. Moreover, the bias-reduced MLE of α and the bias-reduced MME of α are not necessarily better than the MLE of α and the MME of α, respectively, in terms of mean-squared error when the sample size is small. For the percentile estimates, the MLEs of α and β or the MMEs of α and β without bias corrections are used to replace α and β in the formula of percentile W_p.

Ng *et al.*[13] had established the joint asymptotic distribution of $\hat{\alpha}$ and $\hat{\beta}$ and the joint asymptotic distribution of $\tilde{\alpha}$ and $\tilde{\beta}$. Therefore, by using the delta method, the asymptotic distribution for $\hat{W}_p$ and $\tilde{W}_p$ can be obtained for a large sample size. However, it should be mentioned that the sampling distributions for all the estimators mentioned above are not available, nor should the delta method be applied to derive the respective sampling distributions for $\hat{W}_p$ and $\tilde{W}_p$ under a small sample size.

DOI: 10.1002/qre

3. CONSTRUCTION OF A BOOTSTRAP CONTROL CHART

Many authors have studied the application of bootstrap methods to statistical quality control charts. The non-parametric bootstrap method can be applied to control charts, thereby eliminating the traditional parametric assumption. Hence, bootstrap methods can also be applied when the distribution of the statistic used to monitor the process is not available.

Bajgier[14] developed a bootstrap control chart for the process mean, which is a competitor to Shewhart's $\bar{X}$ chart. The only assumption used by Bajgier[14] is that the process is stable and in control when the control limits are computed. If this assumption is not satisfied when the control limits are computed, the limits will be too wide, regardless of the distribution of the process variable. Many papers had indicated that for skewed distributions, bootstrap techniques seemed to have better estimates of the true percentile values on average than Shewhart-type methods. See References[15–17] for more details.

Nichols and Padgett[9] developed a parametric bootstrap control chart for the Weibull percentiles to monitor the process of producing carbon fibers and compared with the Shewhart-type control charts for percentiles of the Weibull distribution, in terms of ARL during the out-of-control process. They found that the proposed parametric bootstrap method could detect the out-of-control process earlier than the Shewhart-type method proposed by Padgett and Spurrier[8].

Durham and Padgett[1] showed that the Birnbaum–Saunders distributions provided better fits to carbon fiber or composite tensile strengths than the Weibull distribution in many situations. Therefore, it is important to construct a control chart for monitoring the process that produces measurements of the Birnbaum–Saunders distribution. To the best of our knowledge, no control chart for the Birnbaum–Saunders distribution has been developed up to date, because the sampling distributions of all the estimators for α and β are unknown under a small sample size. Our interest in this paper is to construct a bootstrap-type control chart for the Birnbaum–Saunders percentiles. The problem we address in this paper falls into the category of using the parametric bootstrap approach. This investigation was motivated in part by the results of Padgett and Tomlinson[18] that parametric bootstrap approaches produce good lower confidence bounds on Birnbaum–Saunders percentiles.

The following steps are used for the construction of the bootstrap control chart for Birnbaum–Saunders percentiles by using the MLEs of α and β, hence, the MLE of population percentile. Given a positive integer k, which is usually between 20 and 30, m, and n_j, $j=1,2,\ldots,k$, where m and n_j $(j=1,2,\ldots,k)$ are small positive integers such as 3, 4, 5, or 6 and n_j could be the same as m for $j=1,2,\ldots,k$:

1. From the in-control and stable process, observe k random samples of each size n_j $(j=1,2,\ldots,k)$ independently assuming that they come from a Birnbaum–Saunders distribution with unknown shape α and scale β. A probability plot proposed by Durham and Padgett[1] for Birnbaum–Saunders should be constructed to check this assumption. Let observations of the jth sample be denoted by x_{ij}, $i=1,\ldots,n_j$.
2. Using Equations (1) and (2), evaluate the MLEs of α and β with the pooled sample of size $N=\sum n_j$ observed. Here a one-dimensional root search is used for solving $\hat{\alpha}$ from Equation (1). The unique positive root is guaranteed within the interval (r,s) as mentioned earlier.
3. Generate a parametric bootstrap sample of size m, $x_1^*, x_2^*, \ldots, x_m^*$ from the Birnbaum–Saunders distribution using the MLEs obtained in Step 2 as the Birnbaum–Saunders distribution parameters. Here, m is the sample size, which will be used for future subgroup samples.
4. Find the parameter MLEs with the bootstrap sample obtained in Step 3 and denote these MLEs by $\hat{\alpha}^*$ and $\hat{\beta}^*$.
5. For the bootstrap sample obtained in Step 3 and the MLEs obtained in Step 4, calculate the bootstrap sample, $\hat{W}_p^* = (\hat{\beta}^*/4)[\hat{\alpha}^* z_p + (\hat{\alpha}^{*2} z_p^2 + 4)^{1/2}]^2$, of the $100p$th percentile $\hat{W}_p = (\hat{\beta}/4)[\hat{\alpha} z_p + (\hat{\alpha}^2 z_p^2 + 4)^{1/2}]^2$, where $z_p = \Phi^{-1}(p)$ is the standard normal $100p$th percentile.
6. Repeat Steps 3–5 a large number of times, B, obtaining B bootstrap samples of $\hat{W}_p$, denoted by $\hat{W}_{p1}^*, \ldots, \hat{W}_{pB}^*$.

DOI: 10.1002/qre

7. Using the B bootstrap samples obtained in Step 6, find the $(\gamma/2)$th and $(1-\gamma/2)$th quantiles. Here, γ is the probability that an observation is considered as out of control when the process is actually in control, i.e. false alarm rate (FAR). These $(\gamma/2)$th and $(1-\gamma/2)$th quantiles are the LCL and UCL for the bootstrap control chart of FAR $=\gamma$, respectively. It should be noted that several versions of the sample quantiles have been suggested in the statistics literature. In the simulation study, we used the method proposed by Hyndman and Fan[19].

The above bootstrap control chart is called the MLE bootstrap control chart. Similarly, if the MLEs of α and β are replaced by the MMEs, $\tilde{\alpha}$ and $\tilde{\beta}$, respectively, and the MLE method is replaced by the MME method in Steps 2–4 of the procedure mentioned above, then the bootstrap control chart is constructed by using the modified moment method. The later bootstrap control chart is called the MME bootstrap control chart.

Once the control limits have been computed, future subgroup samples of size m, which is used as the subgroup size for the construction of the bootstrap control chart, are taken from the process at regular time intervals, and W_p is estimated for each of the new subgroups by the MLE ($\hat{W}_p$) for using the MLE bootstrap control chart or by the MME ($\tilde{W}_p$) for using the MME bootstrap control chart as indicated in Section 2. If the estimate, $\hat{W}_p$ (or $\tilde{W}_p$), falls between the UCL and LCL of the MLE bootstrap control chart (or the MME bootstrap control chart) calculated in Step 7, the process is assumed to be in control. Otherwise, signal that the process may be out of control. Hence, once the bootstrap control limits are found, the process is monitored using the statistic $\hat{W}_p$ (or $\tilde{W}_p$) for W_p in the usual manner.

It should be mentioned that the procedures of the bootstrap quality control charts in this section are based on the following principles:

(i) Use all the in-control subgroup samples of small size (n) to find the MLE (or MME) estimates of the common unknown population parameters α and β. Therefore, the center line (CL), $\hat{W}_p$ (or $\tilde{W}_p$), of the MLE bootstrap control charts (or the MME bootstrap control charts) for the percentiles can be calculated by plugging in the MLE (or MME) estimates of α and β.

(ii) Use the empirical distribution of B bootstrap samples as the approximated sampling distribution of monitoring statistic, $\hat{W}_p$ (or $\tilde{W}_p$), under a small sample size m (which could be the same as n) to create LCL and UCL for the MLE (or MME) bootstrap control charts of the population percentiles.

(iii) The process is monitored by the corresponding statistic, $\hat{W}_p$ (or $\tilde{W}_p$), calculated by using each further subgroup sample of small size m generated from the process.

The process is consistent with the process for Shewhart control charts as well as the process for quality control charts mentioned in the papers. Therefore, the proposed bootstrap control charts are for monitoring for the subgroups of a small sample size (m).

4. SIMULATION STUDY

In this section, computer simulations to check the performance of the bootstrap Birnbaum–Saunders percentile control chart are presented. The simulations were conducted in R language[20], which is a non-commercial, open-source software package for statistical computing and graphics that was originally developed by Ihaka and Gentleman[21]. This can be obtained at no cost from http://www.r-project.org. It is also noteworthy that Leiva *et al.*[22] recently announced the development of a new R package for the Birnbaum–Saunders distribution, which can be conveniently used for computation.

The behavior of the bootstrap control chart for Birnbaum–Saunders percentiles is investigated by calculating the average UCL and LCL and their associated standard errors from simulations. The simulations also examine ARLs and the associated variance for each of the ARLs while the process is in control. The simulations are carried out with different sample sizes, different percentiles of interest, and different levels of FARs for many processes. The ARLs with the associated variances are also computed when the process shifts from in-control to out-of-control.

DOI: 10.1002/qre

The average UCL and LCL and the associated standard errors were computed in the following manner: for each set of k independent samples of size n ($k=20$ samples of the same size were used from the simulations) obtained from a Birnbaum–Saunders distribution with a given scale parameter, α, and a given shape parameter, β as described in Step 1, Steps 2–7 were then carried out with $B=10000$ to generate control limits. This entire process (Steps 1–7) was repeated 10 000 times and the average LCLs and UCLs were computed from the 10 000 generated values of LCLs and UCLs, respectively. The corresponding standard errors of the control limits were also computed from the respective 10 000 values. Some of the simulation results of average LCL and UCL with the corresponding standard errors are given in Tables II and III (sample size 5) and in Tables V and VI (sample size 4) for MLE control charts, and are given in Tables VIII and IX (sample size 5) and in Tables XI and XII (sample size 4) for MME control charts. As one would expect, when the subgroup size n increased, the control limits get closer together, and as the percentile is increased from 0.01 to 0.1 to 0.5, the limits become farther apart for both MLE and MME charts generally. Both MLE and MME control limits behave very similarly.

The in-control ARL was obtained as follows: for each set of $k=20$ samples of the same size, the control limits were established by Steps 2–7. Once the control limits were computed, the further subgroup samples of the same size were continuously generated from the same process and the W_p were estimated by the MLE, $\hat{W}_p$ (or the MME, $\tilde{W}_p$) from the each of further subgroups for using the MLE control chart (or the MME control chart). The number of times needed for the first estimate, $\hat{W}_p$ (or $\tilde{W}_p$), to be out-of-control limits was recorded as the run length for each respective control chart. This entire process of obtaining the run length was replicated 10 000 times and the average of the resulting 10 000 run lengths (ARL) and their standard errors were calculated, respectively.

Some of the results for ARL are listed in Table I (sample size 5) and Table IV (sample size 4) for the MLE charts and are listed in Table VII (sample size 5) and Table X (sample size 4) for the MME charts. On the basis of the standard theory, we expect the reciprocal of the FAR to be the theoretical ARL. For example, when the FAR is 0.0027, we expect the ARL to be equal to 370. Smaller ARL indicates that the control limits computed may typically be too narrow, and ARL larger than 370 indicates that the control limits computed may be too wide or that the bootstrap control charts give fewer false signals. In general, the simulated ARLs were close to the theoretical results, except for the cases of FAR = 0.0027 and 0.002,

Table I. MLE in-control ARL estimate and its corresponding SD for $p=0.01, 0.1, 0.5$ percentiles and $\gamma_0=0.1, 0.01, 0.0027, 0.002$ FARs ($n_j=5$ for $j=1,\ldots,20$ and $m=5$)

Shape parameter	$p=0.01$		$p=0.1$		$p=0.5$	
	ARL	SD	ARL	SD	ARL	SD
	$\gamma_0=0.1$ (FAR)		$1/\gamma_0=10$			
$\alpha=0.5$	9.5810	0.09961524	9.3461	0.09737053	9.2323	0.09161066
$\alpha=1.0$	9.5912	0.09800004	9.5640	0.09844044	9.4406	0.09682802
$\alpha=2.0$	9.4267	0.09327868	9.5552	0.09581802	9.4255	0.09226688
	$\gamma_0=0.01$ (FAR)		$1/\gamma_0=100$			
$\alpha=0.5$	100.3945	1.43446697	97.5134	1.33087577	93.9245	1.18643781
$\alpha=1.0$	100.0540	1.28275408	99.3314	1.32787448	92.9107	1.14414936
$\alpha=2.0$	98.0464	1.19784195	100.7390	1.31357059	91.1806	1.05667712
	$\gamma_0=0.0027$ (FAR)		$1/\gamma_0=370.37$			
$\alpha=0.5$	423.0440	9.37562952	399.1231	6.55707227	368.5128	5.53553116
$\alpha=1.0$	409.6088	6.80627864	413.5364	8.16620935	359.7879	5.64493207
$\alpha=2.0$	379.3317	5.43383492	394.7442	6.05780472	353.4099	5.13447568
	$\gamma_0=0.002$ (FAR)		$1/\gamma_0=500$			
$\alpha=0.5$	596.6028	15.32978642	544.5530	9.04573227	505.4659	8.06874042
$\alpha=1.0$	564.2519	9.21221589	574.2022	11.74351502	495.7047	8.15403660
$\alpha=2.0$	521.9982	7.86818627	550.0370	9.63257838	485.1886	7.91803599

DOI: 10.1002/qre

Table II. MLE in-control LCL and UCL estimates for $p=0.01, 0.1, 0.5$ percentiles and $\gamma_0=0.1, 0.01, 0.0027, 0.002$ FARs ($n_j=5$ for $j=1,\ldots,20$ and $m=5$)

Shape parameter	$p=0.01$		$p=0.1$		$p=0.5$	
	LCL	UCL	LCL	UCL	LCL	UCL
	$\gamma_0=0.1$ (FAR)					
$\alpha=0.5$	0.50992980	1.221284	0.6025905	1.295174	0.7021885	1.427397
$\alpha=1.0$	0.14082786	1.229027	0.2667440	1.442946	0.5194005	1.945590
$\alpha=2.0$	0.01237371	0.949325	0.0374524	1.417540	0.3364735	3.037621
	$\gamma_0=0.01$ (FAR)					
$\alpha=0.5$	0.37820750	1.527583	0.4852428	1.600613	0.5765940	1.739700
$\alpha=1.0$	0.06776361	2.011624	0.1581386	2.247135	0.3619502	2.798443
$\alpha=2.0$	0.00471870	2.967817	0.0150098	3.728595	0.1794053	5.727317
	$\gamma_0=0.0027$ (FAR)					
$\alpha=0.5$	0.32528650	1.687469	0.4390921	1.760735	0.5275497	1.901811
$\alpha=1.0$	0.04886306	2.474309	0.1226165	2.716770	0.3086310	3.285724
$\alpha=2.0$	0.00316629	4.499997	0.0101825	5.360336	0.1378848	7.479096
	$\gamma_0=0.002$ (FAR)					
$\alpha=0.5$	0.31456610	1.723305	0.4298014	1.796520	0.5177948	1.938438
$\alpha=1.0$	0.04556197	2.582617	0.1160812	2.826657	0.2985489	3.398642
$\alpha=2.0$	0.00291175	4.880180	0.0093843	5.757390	0.1307134	7.895151

Table III. The standard deviation of the control limits in Table II ($n_j=5$ for $j=1,\ldots,20$ and $m=5$)

Shape parameter	$p=0.01$		$p=0.1$		$p=0.5$	
	LCL	UCL	LCL	UCL	LCL	UCL
	$\gamma_0=0.1$ (FAR)					
$\alpha=0.5$	0.000456506	0.00059996	0.000414147	0.00065651	0.000381389	0.000772385
$\alpha=1.0$	0.000316447	0.00109575	0.000436161	0.00128627	0.000506800	0.001888290
$\alpha=2.0$	0.000041308	0.00138273	0.000117294	0.00193371	0.000482627	0.004325105
	$\gamma_0=0.01$ (FAR)					
$\alpha=0.5$	0.000453603	0.00084080	0.000401102	0.00092100	0.000355587	0.001071738
$\alpha=1.0$	0.000183260	0.00195855	0.000330371	0.00225205	0.000395322	0.003039545
$\alpha=2.0$	0.000016401	0.00440886	0.000050815	0.00565541	0.000291098	0.009195014
	$\gamma_0=0.0027$ (FAR)					
$\alpha=0.5$	0.000449680	0.00102278	0.000400566	0.00111023	0.000351434	0.001261261
$\alpha=1.0$	0.000141841	0.00267184	0.000285931	0.00299693	0.000360770	0.003824752
$\alpha=2.0$	0.000011286	0.00762353	0.000035655	0.00905379	0.000238856	0.012838680
	$\gamma_0=0.002$ (FAR)					
$\alpha=0.5$	0.000449066	0.00107440	0.000401164	0.00115851	0.000351651	0.001313544
$\alpha=1.0$	0.000134074	0.00285780	0.000277510	0.00319851	0.000355595	0.004023480
$\alpha=2.0$	0.000010411	0.00851063	0.000033174	0.00998354	0.000229995	0.013764536

which showed slightly higher simulated ARLs. However, the simulated ARLs are getting better for lower FAR when the subgroup sample size increases. Again, the simulated ARLs for both MLE and MME charts are similar.

Simulations were also performed to evaluate the performance of the bootstrap control chart monitoring the process being out of control. First, the control limits of the in-control process were established and then the control limits were used to monitor the estimated percentiles $\hat{W}_p$ (for the MLE control chart) or $\tilde{W}_p$

DOI: 10.1002/qre

Table IV. MLE in-control ARL estimate and its corresponding SD for $p=0.01, 0.1, 0.5$ percentiles and $\gamma_0=0.1, 0.01, 0.0027, 0.002$ FARs ($n_j=4$ for $j=1,\ldots,20$ and $m=4$)

Shape parameter	$p=0.01$		$p=0.1$		$p=0.5$	
	ARL	SD	ARL	SD	ARL	SD
	$\gamma_0=0.1$ (FAR)		$1/\gamma_0=10$			
$\alpha=0.5$	9.7521	0.10157930	9.5269	0.10107660	9.5208	0.09848932
$\alpha=1.0$	9.5914	0.09728520	9.4018	0.09827686	9.3681	0.09569000
$\alpha=2.0$	9.7070	0.09830413	9.5341	0.09735436	9.4673	0.09205010
	$\gamma_0=0.01$ (FAR)		$1/\gamma_0=100$			
$\alpha=0.5$	104.4050	1.53582440	100.2868	1.46536560	95.7320	1.36846693
$\alpha=1.0$	103.8034	1.42618970	101.1473	1.42938221	95.1026	1.26739500
$\alpha=2.0$	100.1410	1.30089805	98.9611	1.31255463	94.2245	1.21256610
	$\gamma_0=0.0027$ (FAR)		$1/\gamma_0=370.37$			
$\alpha=0.5$	431.3566	8.31879270	418.7329	8.08162260	397.4719	7.35001283
$\alpha=1.0$	416.0231	7.14014010	424.9688	7.49718875	376.6396	6.15565200
$\alpha=2.0$	402.2870	6.41209024	410.0969	7.59334126	365.7644	5.78346700
	$\gamma_0=0.002$ (FAR)		$1/\gamma_0=500$			
$\alpha=0.5$	614.2333	13.06739560	591.6370	13.01761530	547.5608	10.81352911
$\alpha=1.0$	587.9349	10.62430360	608.5125	12.54152983	523.2881	9.11827300
$\alpha=2.0$	558.2460	9.48296592	580.4710	11.47549614	497.7902	8.07272630

Table V. MLE in-control LCL and UCL estimates for $p=0.01, 0.1, 0.5$ percentiles and $\gamma_0=0.1, 0.01, 0.0027, 0.002$ FARs ($n_j=4$ for $j=1,\ldots,20$ and $m=4$)

Shape parameter	$p=0.01$		$p=0.1$		$p=0.5$	
	LCL	UCL	LCL	UCL	LCL	UCL
	$\gamma_0=0.1$ (FAR)					
$\alpha=0.5$	0.49560530	1.295198	0.5831981	1.363483	0.6745071	1.487898
$\alpha=1.0$	0.13600010	1.423391	0.2555557	1.628370	0.4799941	2.107869
$\alpha=2.0$	0.01210842	1.410623	0.0363066	1.929202	0.2895728	3.549476
	$\gamma_0=0.01$ (FAR)					
$\alpha=0.5$	0.35464050	1.655193	0.4588600	1.723163	0.5420152	1.854222
$\alpha=1.0$	0.06028494	2.401455	0.1434527	2.625593	0.3221960	3.151869
$\alpha=2.0$	0.00416956	4.337389	0.0132199	5.113503	0.1469215	7.052933
	$\gamma_0=0.0027$ (FAR)					
$\alpha=0.5$	0.29867910	1.845617	0.4107898	1.913314	0.4914405	2.046576
$\alpha=1.0$	0.04190480	2.983076	0.1079206	3.214565	0.2710756	3.755856
$\alpha=2.0$	0.00269540	6.423053	0.0086434	7.273654	0.1119803	9.303239
	$\gamma_0=0.002$ (FAR)					
$\alpha=0.5$	0.28743640	1.888792	0.4011763	1.956634	0.4812320	2.090136
$\alpha=1.0$	0.03880224	3.119578	0.1014038	3.351845	0.2614094	3.896238
$\alpha=2.0$	0.00246421	6.927375	0.0079123	7.794370	0.1060421	9.838039

(for the MM control chart) calculated from the further subgroup sample generated from the out-of-control process by increasing the parameter α. It should be noted that Chang and Tang[23] have showed W_p to be a decreasing function with respect to α when $p \leq 0.5$ graphically. Our main concern is specifically with small percentiles. A downward shift in a lower percentile of the strength distribution indicates a decrease

DOI: 10.1002/qre

Table VI. The standard deviation of the control limits in Table V ($n_j = 4$ for $j = 1, \ldots, 20$ and $m = 4$)

Shape parameter	$p = 0.01$		$p = 0.1$		$p = 0.5$	
	LCL	UCL	LCL	UCL	LCL	UCL
	$\gamma_0 = 0.1$ (FAR)					
$\alpha = 0.5$	0.000490865	0.00071890	0.000449797	0.00078769	0.000417477	0.000920888
$\alpha = 1.0$	0.000341059	0.00143323	0.000464457	0.00166405	0.000535654	0.002341127
$\alpha = 2.0$	0.000044580	0.00213802	0.000125526	0.00288507	0.000482882	0.005776521
	$\gamma_0 = 0.01$ (FAR)					
$\alpha = 0.5$	0.000487016	0.00106916	0.000432702	0.00115898	0.000388028	0.001333346
$\alpha = 1.0$	0.000183847	0.00275784	0.000339843	0.00310402	0.000408901	0.003990147
$\alpha = 2.0$	0.000016013	0.00755075	0.000049983	0.00902089	0.000280880	0.013090663
	$\gamma_0 = 0.0027$ (FAR)					
$\alpha = 0.5$	0.000478441	0.00131893	0.000431921	0.00141947	0.000381063	0.001598761
$\alpha = 1.0$	0.000136992	0.00378482	0.000287994	0.00417551	0.000368232	0.005118119
$\alpha = 2.0$	0.000010566	0.01235376	0.000033714	0.01399425	0.000227374	0.018412412
	$\gamma_0 = 0.002$ (FAR)					
$\alpha = 0.5$	0.000476967	0.00138366	0.000431524	0.00148601	0.000380024	0.001666675
$\alpha = 1.0$	0.000128695	0.00405241	0.000277483	0.00445503	0.000361501	0.005404701
$\alpha = 2.0$	0.000009749	0.01357635	0.000031117	0.01527489	0.000218485	0.019715196

Table VII. The MM in-control ARL estimate and its corresponding SD for $p = 0.01, 0.1, 0.5$ percentiles and $\gamma_0 = 0.1, 0.01, 0.0027, 0.002$ FARs ($n_j = 5$ for $j = 1, \ldots, 20$ and $m = 5$)

Shape parameter	$p = 0.01$		$p = 0.1$		$p = 0.5$	
	ARL	SD	ARL	SD	ARL	SD
	$\gamma_0 = 0.1$ (FAR)		$1/\gamma_0 = 10$			
$\alpha = 0.5$	9.4168	0.09707116	9.3745	0.09700003	9.3386	0.09452930
$\alpha = 1.0$	9.5893	0.09846305	9.4689	0.09942138	9.2427	0.09218215
$\alpha = 2.0$	9.5651	0.09444357	9.6346	0.09589321	9.3072	0.09135928
	$\gamma_0 = 0.01$ (FAR)		$1/\gamma_0 = 100$			
$\alpha = 0.5$	100.5904	1.41326481	96.3830	1.29763308	95.8458	1.2482204
$\alpha = 1.0$	101.1404	1.34556634	98.6620	1.43340850	93.0184	1.1517089
$\alpha = 2.0$	97.3276	1.16978776	100.8244	1.33548118	91.9876	1.0808889
	$\gamma_0 = 0.0027$ (FAR)		$1/\gamma_0 = 370.37$			
$\alpha = 0.5$	407.8263	7.1146856	397.1971	6.70914097	369.6336	5.5191158
$\alpha = 1.0$	413.6725	6.9883355	404.9751	6.79456862	360.0463	5.5915928
$\alpha = 2.0$	377.1671	5.5635139	398.5963	6.38527914	355.1965	5.1232719
	$\gamma_0 = 0.002$ (FAR)		$1/\gamma_0 = 500$			
$\alpha = 0.5$	582.1413	11.3931998	550.1305	9.89180214	511.6485	8.3179301
$\alpha = 1.0$	576.8354	9.8721688	561.3378	9.60096351	492.9208	7.8490585
$\alpha = 2.0$	518.0102	7.7649046	557.4775	9.34762625	488.4649	7.4558382

in the tensile strength (worse quality with respect to tensile strength). Therefore, the only consideration of the out-of-control process for small percentiles is increasing the shape parameter α to decrease W_p.

Twenty samples of size 5 (i.e. $n_j = 5$ for $j = 1, \ldots, 20$) were generated from an in-control process and control limits were calculated by Steps 2–7. Further subgroup samples, each of size $m = 5$, were simulated from a Birnbaum–Saunders distribution with an increased α to shift the out-of-control process. The percentile

DOI: 10.1002/qre

Table VIII. MM in-control LCL and UCL estimates for $p=0.01, 0.1, 0.5$ percentiles and $\gamma_0=0.1, 0.01, 0.0027, 0.002$ FARs ($n_j=5$ for $j=1,\ldots,20$ and $m=5$)

Shape parameter	$p=0.01$		$p=0.1$		$p=0.5$	
	LCL	UCL	LCL	UCL	LCL	UCL
	$\gamma_0=0.1$ (FAR)					
$\alpha=0.5$	0.50985820	1.221396	0.6027699	1.295436	0.7023180	1.427980
$\alpha=1.0$	0.14088391	1.228206	0.2670795	1.442621	0.5198061	1.945194
$\alpha=2.0$	0.01265992	0.953165	0.0379382	1.422357	0.3352013	3.044047
	$\gamma_0=0.01$ (FAR)					
$\alpha=0.5$	0.37813130	1.527763	0.4854331	1.600875	0.5766596	1.740559
$\alpha=1.0$	0.06814989	2.010441	0.1589948	2.246441	0.3623085	2.797082
$\alpha=2.0$	0.00497666	2.977278	0.0156825	3.743361	0.1791324	5.726490
	$\gamma_0=0.0027$ (FAR)					
$\alpha=0.5$	0.3251946	1.687707	0.4393261	1.760885	0.5276459	1.902762
$\alpha=1.0$	0.0493245	2.473249	0.1240010	2.716273	0.3090034	3.283730
$\alpha=2.0$	0.0034227	4.513934	0.0109110	5.382561	0.1378200	7.469652
	$\gamma_0=0.002$ (FAR)					
$\alpha=0.5$	0.3145302	1.723842	0.4300310	1.796630	0.5178262	1.939499
$\alpha=1.0$	0.0461000	2.581797	0.1174794	2.826152	0.2989072	3.396735
$\alpha=2.0$	0.0031710	4.893995	0.0101298	5.783323	0.1306642	7.883126

Table IX. The standard deviation of the control limits in Table VIII ($n_j=5$ for $j=1,\ldots,20$ and $m=5$)

Shape parameter	$p=0.01$		$p=0.1$		$p=0.5$	
	LCL	UCL	LCL	UCL	LCL	UCL
	$\gamma_0=0.1$ (FAR)					
$\alpha=0.5$	0.000451351	0.00059697	0.000411146	0.00065705	0.000382422	0.000776050
$\alpha=1.0$	0.000311670	0.00110208	0.000437255	0.00129563	0.000508047	0.001877682
$\alpha=2.0$	0.000040815	0.00140592	0.000113943	0.00196403	0.000490438	0.004354898
	$\gamma_0=0.01$ (FAR)					
$\alpha=0.5$	0.000448444	0.00083428	0.000393187	0.00091669	0.000356703	0.001077340
$\alpha=1.0$	0.000180157	0.00197486	0.000329711	0.00226515	0.000397280	0.003021706
$\alpha=2.0$	0.000016599	0.00452924	0.000050439	0.00575955	0.000296404	0.009194645
	$\gamma_0=0.0027$ (FAR)					
$\alpha=0.5$	0.000444009	0.00101462	0.000396024	0.00110156	0.000351073	0.001267561
$\alpha=1.0$	0.000138524	0.00272188	0.000285596	0.00301981	0.000362034	0.003799363
$\alpha=2.0$	0.000011614	0.00778131	0.000036340	0.00925384	0.000243280	0.012795156
	$\gamma_0=0.002$ (FAR)					
$\alpha=0.5$	0.000443890	0.00106611	0.000395886	0.00114799	0.000351071	0.001320891
$\alpha=1.0$	0.000131330	0.00291946	0.000276312	0.00322592	0.000356158	0.004004899
$\alpha=2.0$	0.000010817	0.00868596	0.000033920	0.01019537	0.000235298	0.013725578

estimate, $\hat{W}_p$, (or $\tilde{W}_p$) was calculated for each further subgroup. The number of further subgroups needed for the first time $\hat{W}_p$ (or $\tilde{W}_p$) is out of control was recorded as the run length. Again, the entire process of obtaining the run length was replicated 10 000 times, and the ARLs and standard errors were calculated from the 10 000 generated run lengths. As the study showed that the simulated ARLs for in-control were larger than theoretical values for lower FAR, we particularly examined the out-of-control ARLs for FAR = 0.0027.

DOI: 10.1002/qre

Table X. The MM in-control ARL estimate and its corresponding SD for $p=0.01, 0.1, 0.5$ percentiles and $\gamma_0=0.1, 0.01, 0.0027, 0.002$ FARs ($n_j=5$ for $j=1,\ldots,20$ and $m=4$)

Shape parameter	$p=0.01$		$p=0.1$		$p=0.5$	
	ARL	SD	ARL	SD	ARL	SD
	$\gamma_0=0.1$ (FAR)		$1/\gamma_0=10$			
$\alpha=0.5$	9.8441	0.10379920	9.4152	0.10000950	9.5879	0.09889662
$\alpha=1.0$	9.6442	0.09768641	9.4739	0.10041110	9.3444	0.09479450
$\alpha=2.0$	9.5094	0.09426335	9.3768	0.09470966	9.5853	0.09528757
	$\gamma_0=0.01$ (FAR)		$1/\gamma_0=100$			
$\alpha=0.5$	102.3958	1.49006100	97.1817	1.41422340	96.6126	1.3995356
$\alpha=1.0$	100.5846	1.41647482	104.2179	1.57878580	92.5310	1.2615733
$\alpha=2.0$	100.7708	1.40913543	102.6606	1.42952911	92.7867	1.1628300
	$\gamma_0=0.0027$ (FAR)		$1/\gamma_0=370.37$			
$\alpha=0.5$	427.2553	8.1012404	411.8529	8.38671110	404.6409	8.3285458
$\alpha=1.0$	415.3745	7.7217181	437.6863	8.54022320	376.0527	6.3508656
$\alpha=2.0$	399.5726	6.5957727	410.3835	7.42708289	371.9434	6.1313024
	$\gamma_0=0.002$ (FAR)		$1/\gamma_0=500$			
$\alpha=0.5$	595.5793	11.4251646	583.3256	13.4552529	553.8622	10.9268615
$\alpha=1.0$	566.3763	10.7574343	603.7501	11.8948651	522.9515	9.9607332
$\alpha=2.0$	554.4366	9.7192595	588.3330	11.5113843	511.4659	8.7307212

Table XI. MM in-control LCL and UCL estimates for $p=0.01, 0.1, 0.5$ percentiles and $\gamma_0=0.1, 0.01, 0.0027, 0.002$ FARs ($n_j=5$ for $j=1,\ldots,20$ and $m=4$)

Shape parameter	$p=0.01$		$p=0.1$		$p=0.5$	
	LCL	UCL	LCL	UCL	LCL	UCL
	$\gamma_0=0.1$ (FAR)					
$\alpha=0.5$	0.49513360	1.295728	0.5829352	1.361424	0.6745984	1.488979
$\alpha=1.0$	0.13711106	1.422550	0.2569866	1.632428	0.4808776	2.106498
$\alpha=2.0$	0.01241051	1.409964	0.0371320	1.931556	0.2891798	3.570654
	$\gamma_0=0.01$ (FAR)					
$\alpha=0.5$	0.35415000	1.656399	0.4588221	1.720008	0.542002	1.855930
$\alpha=1.0$	0.06127177	2.396724	0.1451099	2.631256	0.323018	3.147984
$\alpha=2.0$	0.00441692	4.327883	0.0139912	5.114312	0.146767	7.091670
	$\gamma_0=0.0027$ (FAR)					
$\alpha=0.5$	0.2982414	1.847082	0.4108135	1.909734	0.4914122	2.048559
$\alpha=1.0$	0.0428795	2.975921	0.1098527	3.220740	0.2718597	3.749757
$\alpha=2.0$	0.0029329	6.407933	0.0093961	7.272365	0.1118735	9.353041
	$\gamma_0=0.002$ (FAR)					
$\alpha=0.5$	0.2869893	1.890296	0.4011741	1.952991	0.4811940	2.092270
$\alpha=1.0$	0.0397983	3.111940	0.1034525	3.358149	0.2621655	3.890791
$\alpha=2.0$	0.0026984	6.909484	0.0086581	7.793333	0.1058882	9.889457

Part of the simulated ARL results after the process was shifted to the out-of-control condition is shown in Table XIII. It can be seen that all ARLs after the process shifts to out of control were uniformly far smaller than the theoretical ARL = 370 for both MLE and MME charts.

DOI: 10.1002/qre

Table XII. The standard deviation of the control limits in Table XI ($n_j = 5$ for $j = 1, \ldots, 20$ and $m = 4$)

Shape parameter	$p = 0.01$		$p = 0.1$		$p = 0.5$	
	LCL	UCL	LCL	UCL	LCL	UCL
	$\gamma_0 = 0.1$ (FAR)					
$\alpha = 0.5$	0.000494044	0.00071770	0.000452490	0.00078193	0.000414933	0.000915436
$\alpha = 1.0$	0.000347579	0.00142084	0.000469216	0.00169453	0.000538121	0.002345702
$\alpha = 2.0$	0.000045667	0.00221815	0.000128350	0.00296155	0.000492944	0.005917483
	$\gamma_0 = 0.01$ (FAR)					
$\alpha = 0.5$	0.000488053	0.00106500	0.000434063	0.00114622	0.000387529	0.001329198
$\alpha = 1.0$	0.000187963	0.00272630	0.000341970	0.00316565	0.000411417	0.003983579
$\alpha = 2.0$	0.000016761	0.00776681	0.000052241	0.00912077	0.000284883	0.013296974
	$\gamma_0 = 0.0027$ (FAR)					
$\alpha = 0.5$	0.000477860	0.00130841	0.000432363	0.00139657	0.000380288	0.001594488
$\alpha = 1.0$	0.000139906	0.00375130	0.000287927	0.00423648	0.000373074	0.005124655
$\alpha = 2.0$	0.000011358	0.01260030	0.000036027	0.01413814	0.000230705	0.018593858
	$\gamma_0 = 0.002$ (FAR)					
$\alpha = 0.5$	0.000476149	0.00137153	0.000432396	0.00146498	0.000379557	0.001663321
$\alpha = 1.0$	0.000131470	0.00401515	0.000277834	0.00451307	0.000366386	0.005406583
$\alpha = 2.0$	0.000010527	0.01387011	0.000033450	0.01543067	0.000221382	0.019908108

Table XIII. Out-of-control ARLs and standard errors with α_1 shift to α_2 ($n_j = 5$ for $j = 1, \ldots, 20$ and $m = 5$)

Percentile	α_1	α_2	ARL_{MLE}	ARL_{MLE} (SE)	ARL_{MME}	ARL_{MME} (SE)
	$\gamma_0 = 0.0027$ (FAR)					
$p = 0.01$	2.0	3.0	13.6649	0.17009784	12.4307	0.14690152
$p = 0.10$	1.0	1.5	11.8470	0.14359151	11.7298	0.13837852
$p = 0.01$	0.5	1.0	3.1776	0.02846800	3.1766	0.02845386
$p = 0.50$	0.5	1.0	8.8563	0.0865519	8.9883	0.08929207
	$\gamma_0 = 0.002$ (FAR)					
$p = 0.01$	2.0	3.0	15.8106	0.20180725	14.2752	0.17515300
$p = 0.10$	1.0	1.5	13.4870	0.16500917	13.4457	0.16669704
$p = 0.01$	0.5	1.0	3.3720	0.03063585	3.3720	0.03027959
$p = 0.50$	0.5	1.0	9.8165	0.09794581	9.9084	0.09954985
	$\gamma_0 = 0.1$ (FAR)					
$p = 0.01$	2.0	3.0	2.6926	0.02268660	2.6660	0.02217101
$p = 0.10$	1.0	1.5	2.6029	0.02124821	2.5839	0.02185003
$p = 0.01$	0.5	1.0	1.6034	0.01010550	1.6027	0.01014473
$p = 0.50$	0.5	1.0	2.5842	0.02038462	2.6254	0.02130711
	$\gamma_0 = 0.01$ (FAR)					
$p = 0.01$	2.1	3.0	7.3157	0.07919262	7.0944	0.07573389
$p = 0.10$	1.0	1.5	6.6469	0.06996536	6.6668	0.07069878
$p = 0.01$	0.5	1.0	2.4559	0.02010786	2.4464	0.01964819
$p = 0.50$	0.5	1.0	5.1752	0.05347144	5.8080	0.05502505

5. ILLUSTRATIVE EXAMPLES

In this section, a process for producing the 6061-T6 aluminum sheeting at Boeing Aircraft Company will be simulated as an example to illustrate the proposed bootstrap control charts for monitoring the breaking

DOI: 10.1002/qre

strength of the aluminum material. The method of observing the strength of 6061-T6 aluminum was described in detail by Birnbaum and Saunders[2,4] and Onar and Padgett[24]. Three data sets from the experiment were reported and studied by Birnbaum and Saunders[2,4]. They fitted the proposed model (the Birnbaum–Saunders fatigue life distribution) to each of the three data sets separately and achieved good fits. The reported data sets were not for the purpose of constructing quality control charts originally and the data were rearranged to sort the data in an increasing order. Thus, the reported data sets cannot be used directly. In this example, The first data set of size 101 was transformed to units of hundreds of thousands of cycles to failure and was used to estimate the parameters of the Birnbaum–Saunders model for strength of the material as the true population parameters input for the in-control process. Twenty subgroups of size 5 strength measurements were simulated independently from this in-control process with the Birnbaum–Saunders model with $\alpha = 0.2795$ and $\beta = 1.358$ (and thus, the first percentile $W_{0.01} = 1.24008$). These 20 in-control subgroups are reported in Table XIV.

5.1. *MLE bootstrap control charts*

The MLE bootstrap control chart for the Birnbaum–Saunders percentile with FAR = 0.0027 was established by utilizing these 20 subgroups in Table XIV from the in-control process following Steps 2–7 with $B = 10000$ and the LCL and UCL were calculated. The CL, $\hat{W}_p$, was calculated by using the same 20 subgroup samples in Table XIV from the in-control process.

Assume that after the process had shifted to an out-of-control process that had a different shape parameter $\alpha = 0.8782$ (and thus, the first percentile, $W_{0.01} = 0.5693$, for the out-of-control process), further subgroups of size 5 from the out-of-control process were simulated for monitoring purpose and are reported in Table XV. Figure 1 shows the LCL (0.9155) and UCL (1.8740) of the MLE bootstrap control chart for the first percentile of the Birnbaum–Saunders model under the in-control process, and another 20 first percentile statistics from the out-of-control process. The CL is also superimposed in the figure. The MLE bootstrap control chart with the CL indicates that the sampling distribution for the first percentile of the Birnbaum–Saunders distribution is not symmetric. It can be seen clearly that the process has immediately signaled out of control and only 6 points out of the 20 points are within the limits and 1 point above the CL.

Table XIV. First 20 in-control subgroups

Subgroup	Breaking stress of 6061-T6 aluminum				
1	1.1400	1.4300	1.0760	2.1130	1.4890
2	1.0800	1.5560	1.6690	1.5950	1.2470
3	2.0660	1.5140	1.1420	0.7382	1.8570
4	1.3410	1.3520	1.7670	1.7080	1.6030
5	1.7540	1.6890	1.3870	0.7842	1.6150
6	1.3370	1.3000	0.9028	1.1880	1.5260
7	1.9810	1.3200	1.5130	1.3380	0.9263
8	1.2090	1.2160	1.3360	1.8450	1.6800
9	1.2970	1.2650	1.6500	1.5860	1.1210
10	1.1150	1.5040	1.6830	1.3160	1.7360
11	1.5180	1.1450	1.4940	0.9917	2.0220
12	2.3460	1.2260	1.0150	1.5920	1.3080
13	2.6250	1.3430	1.6460	1.3690	1.1040
14	1.4320	0.8243	2.0400	1.4170	2.4700
15	1.5510	1.1140	1.6100	1.0470	0.9583
16	1.4730	1.2000	1.3580	1.3870	1.1520
17	1.1590	1.3080	1.8850	0.8899	1.6030
18	1.4900	1.8260	1.2470	1.5060	1.4630
19	1.1670	1.9000	1.8760	1.6510	2.1080
20	1.5870	0.9522	1.1570	0.9660	1.1900

Shape parameter $\alpha = 0.2795$ and scale parameter $\beta = 1.358$ ($W_{0.01} = 1.24$).

DOI: 10.1002/qre

Table XV. Second 20 subgroups after-process shift

Subgroup	Breaking stress of 6061-T6 aluminum				
21	0.2802	8.5320	0.6270	0.7666	0.4136
22	0.5193	1.2900	1.6890	2.0510	1.5920
23	2.3440	0.7174	1.3840	0.8069	4.2170
24	0.4155	3.1470	0.5654	1.0830	0.7527
25	1.5110	1.6880	0.3693	2.5640	0.5355
26	0.2187	0.7716	1.1730	0.8068	1.6490
27	1.4360	3.9910	0.9569	1.3440	1.9070
28	1.7260	0.7707	5.8540	1.6310	3.0470
29	0.9880	0.8541	7.2170	3.6320	1.2210
30	4.5620	1.1860	4.4480	1.5750	0.5950
31	4.4740	0.4357	2.3460	0.4436	0.5680
32	0.5459	1.1980	2.1900	3.8360	2.0280
33	0.4348	1.1260	5.9990	1.1450	1.1550
34	1.7790	0.7027	1.2210	3.0870	0.5239
35	1.9460	0.5319	2.6140	1.3990	5.2110
36	2.2010	0.6235	4.5500	0.8861	1.3870
37	0.5653	3.5950	1.4090	0.3026	0.7666
38	1.5310	1.3910	1.6390	3.1030	2.9400
39	0.5322	0.7735	0.8168	0.5365	5.0100
40	1.4360	1.1170	1.0440	1.0380	0.8156

Shape parameter $\alpha = 0.8782$ and scale parameter $\beta = 1.358$ ($W_{0.01} = 0.5693$).

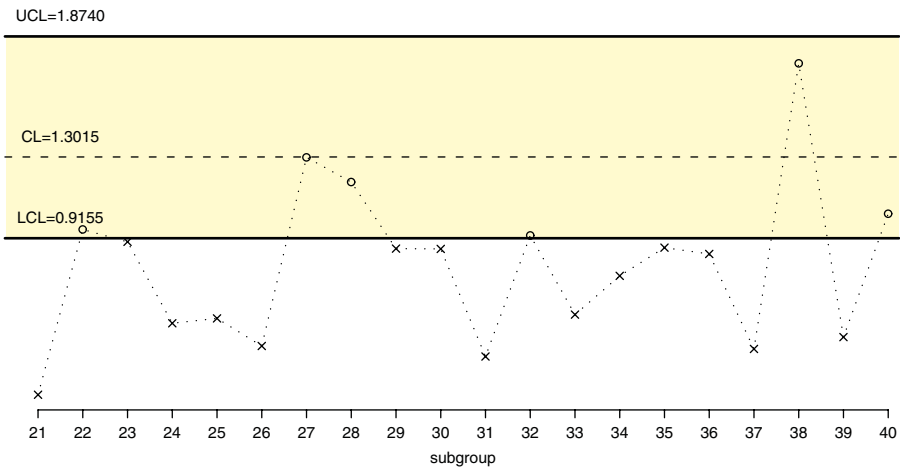

Figure 1. MLE bootstrap control chart based on 20 subgroups with FAR $\gamma_0 = 0.0027$

5.2. *MME bootstrap control charts*

Similarly, the MME bootstrap control chart for the Birnbaum–Saunders percentile with FAR = 0.0027 can be established through the same process but using the MME method instead of the MLE method. Figure 2 shows the LCL (0.9156) and UCL (1.8740) of the MME bootstrap control chart for the first percentile of the Birnbaum–Saunders model. The CL, $\tilde{W}_p$, was calculated by the MME method with all 20 subgroup samples in Table XIV from the in-control process. It can be seen that the MME bootstrap control chart is almost the same as the MLE bootstrap control chart.

DOI: 10.1002/qre

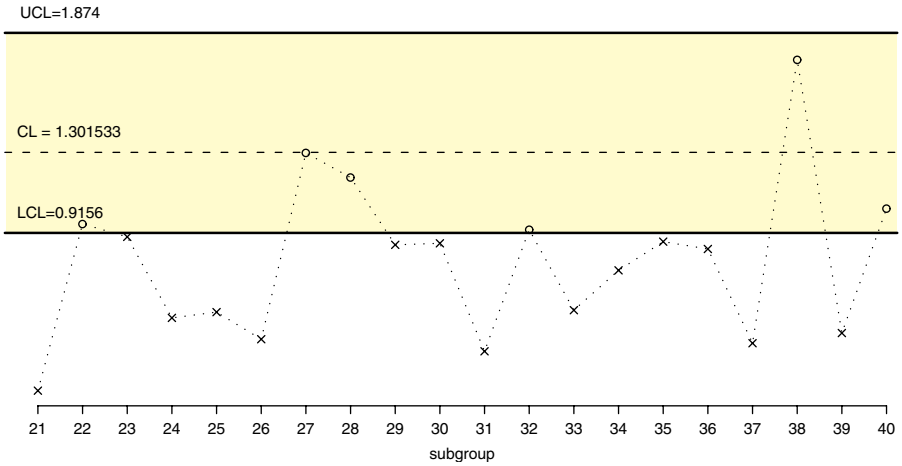

Figure 2. MME bootstrap control chart based on 20 subgroups with FAR $\gamma_0 = 0.0027$

6. CONCLUDING REMARKS

Parametric bootstrap control charts based on MLE and MME are proposed for monitoring percentiles of the Birnbaum–Saunders probability models. Through the extensive Monte Carlo simulations, we showed that the control limits for both MLE and MME charts could be established accurately for Birnbaum–Saunders percentiles by the proposed parametric bootstrap method and both MLE charts and MME charts behave very similarly. Using the MME method, the root search for solving nonlinear equation (1) can be avoided. Therefore, the advantage of using the MME chart over the MLE chart is time saving for the construction of LCL and UCL. The proposed parametric bootstrap control limits (MLE chart or MME chart) signals out of control quickly. Therefore, the parametric bootstrap control charts, either MLE charts or MME charts, should be used instead of the Shewhart-type control chart for the Birnbaum–Saunders percentile as the sampling distribution of the required statistic of the Birnbaum–Saunders percentile is not tractable for small sample size and is generally asymmetric.

Acknowledgements

The authors thank Professor W. J. Padgett of Statistics at the University of South Carolina and of Mathematical Sciences at Clemson University for reading this article and providing helpful comments.

REFERENCES

1. Durham SD, Padgett WJ. A cumulative damage model for system failure with application to carbon fibers and composites. *Technometrics* 1997; **39**:34–44.
2. Birnbaum ZW, Saunders SC. A statistical model for life length of material. *Journal of the American Statistical Association* 1958; **53**:151–160.
3. Birnbaum ZW, Saunders SC. A new family of life distributions. *Journal of Applied Probability* 1969; **6**:319–327.
4. Birnbaum ZW, Saunders SC. Estimation for a family of life distributions with applications to fatigue. *Journal of Applied Probability* 1969; **6**:328–347.
5. Efron B, Tibshirani RJ. *An Introduction to the Bootstrap*. Chapman & Hall: New York, 1993.
6. Gunter B. Bootstrapping: How to make something from almost nothing and get statistically valid answers, part III. *Quality Progress* 1992; **25**:119–122.
7. Young GA. Bootstrap: More than a stab in the dark. *Statistical Science* 1994; **9**:382–415.

DOI: 10.1002/qre

8. Padgett WJ, Spurrier JD. Shewhart-type charts for percentiles of strength distributions. *Journal of Quality Technology* 1990; **22**:283–288.
9. Nichols MD, Padgett WJ. A bootstrap control chart for Weibull percentiles. *Quality and Reliability Engineering International* 2005; **22**:141–151.
10. Tagaras G. Economic $\bar{X}$ charts with asymmetric control limits. *Journal of Quality Technology* 1989; **21**:147–154.
11. Marcellus RL. Performance measures for $\bar{X}$ charts with asymmetric control limits. *Quality and Reliability Engineering International* 2006; **22**:481–491.
12. Engelhardt M, Bain LJ, Wright FT. Inferences on the parameters of the Birnbaum–Saunders fatigue life distribution based on the maximum likelihood estimation. *Technometrics* 1981; **23**:251–256.
13. Ng HKT, Kundu D, Balakrishnan N. Modified moment estimation for the two-parameter Birnbaum–Saunders distribution. *Computational Statistics & Data Analysis* 2002; **43**:283–298.
14. Bajgier SM. The use of bootstrapping to construct limits on control charts. *Proceedings of the Decision Science Institute*, San Diego, CA, 1992; 1611–1613.
15. Seppala T, Moskowitz H, Plante R, Tang J. Statistical process control via the subgroup bootstrap. *Journal of Quality Technology* 1996; **27**:139–153.
16. Liu RY, Tang J. Control charts for dependent and independent measurements based on the bootstrap. *Journal of the American Statistical Association* 1996; **91**:1694–1700.
17. Jones LA, Woodall WY. The performance of bootstrap control charts. *Journal of Quality Technology* 1998; **30**:362–375.
18. Padgett WJ, Tomlinson MA. Lower confidence bounds for percentiles of Weibull and Birnbaum–Saunders distributions. *Journal of Statistical Computation and Simulation* 2003; **73**:429–443.
19. Hyndman RJ, Fan Y. Sample quantiles in statistical packages. *American Statistician* 1996; **50**:361–365.
20. R Development Core Team. *R*: *A Language and Environment for Statistical Computing*. R Foundation for Statistical Computing: Vienna, Austria, 2008. Available at: http://www.R-project.org. ISBN 3-900051-07-0.
21. Ihaka R, Gentleman R. R: A language for data analysis and graphics. *Journal of Computational and Graphical Statistics* 1996; **5**:299–314.
22. Leiva V, Hernández H, Riquelme M. A new package for the Birnbaum–Saunders distribution. *R News* 2006; **6**(4):35–40. Available at: http://CRAN.R-project.org/doc/Rnews/.
23. Chang DS, Tang LC. Percentile bounds and tolerance limits for the Birnbaum–Saunders distribution. *Communications in Statistics*, *Part A—Theory and Methods* 1994; **23**(10):2853–2863.
24. Onar A, Padgett WJ. Inverse Gaussian accelerated test models based on cumulative damage. *Journal of Statistical Computation and Simulation* 2000; **66**:233–247.

Authors' biographies

Yuhlong Lio is a Professor in the Department of Mathematical Sciences at the University of South Dakota. His research interests include reliability, smooth estimator, survival analysis and Statistical process control. He received his BS in Mathematics from National Cheng-Kung University, his MS in Mathematics from National Center University and his PhD in statistics from the University of South Carolina in 1987.

Chanseok Park is an Associate Professor of Mathematical Sciences at Clemson University, Clemson, SC. He received his BS in Mechanical Engineering from Seoul National University, his MA in Mathematics from the University of Texas at Austin and his PhD in Statistics in 2000 from Pennsylvania State University. His research interests include statistical process control, minimum distance estimation, survival and reliability analysis, statistical computing and simulation, acoustics and solid mechanics.

DOI: 10.1002/qre